Received: 9 January 2024 | Revised: 16 March 2024 | Accepted: 30 March 2024

IET Generation, Transmission & Distribution

DOI: 10.1049/gtd2.13169

The Institution of Engineering and Technology WILEY

ORIGINAL RESEARCH

Enhancing DC microgrid performance through machine learning-optimized droop control

Younes Saeidinia[1] | **Mohammadreza Arabshahi**[1] | **Mohammad Aminirad**[2] | **Miadreza Shafie-khah**[3]

[1]Faculty of Electrical Engineering, Shahid Beheshti University, Tehran, Iran

[2]Faculty of Technology and Engineering, Iran University of Science and Technology (IUST), Tehran, Iran

[3]School of Technology and Innovations, University of Vaasa, Vaasa, Finland

Correspondence
Younes Saeidinia, Faculty of Electrical Engineering, Shahid Beheshti University, AC, Tehran, Iran.
Email: y.saeidiniya@alumni.sbu.ac.ir

Abstract

A machine learning-based optimized droop method is suggested here to simultaneously reduce the production cost (PC) and power line losses (PLL) for a class of direct current (DC) microgrids (MGs). Traditionally, a communication-less technique known as the hybrid droop method has been employed to decrease PC and PLL in DC MGs. However, achieving the desired reduction in either PC or PLL requires arbitrary adjustments of weighting coefficients for each distributed generator in the conventional hybrid droop method. To address this challenge, this paper introduces a systematic approach that capitalizes on the benefits of artificial intelligence to accurately predict both the PC and PLL in a DC MG. Furthermore, an optimization technique relying on the gradient descendent method is employed to independently optimize both PC and PLL for each scenario. The effectiveness of the proposed method is confirmed through a comparative study with classical and hybrid droop coordination schemes under various scenarios such as rapid load changes.

1 | INTRODUCTION

Renewable energies, including solar, wind, hydro, and biomass, are sources of electricity generation that do not rely on fossil fuels [1]. By replacing carbon-intensive energy sources, they play a crucial role in significantly mitigating greenhouse gas emissions and addressing climate change. The transition to renewable energy is essential for achieving global climate targets, as outlined in agreements like the Paris Agreement. In this context, microgrids (MGs) offer a promising architecture to meet the zero-carbon targets.

MGs are generally classified into three types: direct current (DC) MGs, AC MGs, and hybrid [2]. Among these, DC MGs have gained considerable interest due to their distinctive features. A DC MG typically incorporates local energy sources, such as solar panels, wind turbines, batteries, or fuel cells, along with loads and energy storage devices. The MG can be interconnected with the main power grid or operate autonomously, providing electricity to a specific area or building [3].

While DC MGs offer promising advantages, including efficiency, reliability, and incorporation of renewable energy, they also encounter challenges, particularly when there is a substantial increase in the penetration of renewable energy sources (RESs). These challenges arise from the need to effectively manage and control the fluctuating nature of renewable energy generation within the MG. The intermittent nature of renewable sources can lead to voltage fluctuations, necessitating the implementation of advanced control and power management systems to maintain stability and ensure grid reliability. To design a suitable power management strategy in the presence of various distributed generations (DGs), many attempts have been made by the researchers.

Some researchers have explored control plans to ensure the efficient, coordinated, and reliable operation of multiple RESs and ESSs. The focus of these control strategies is to optimize the distribution of loads and minimize generation costs, particularly when aiming for cost-effective operation and determining the most suitable combination of dispatchable and non-dispatchable DG units. Consequently, researchers are motivated to include an economic dispatch as part of their control measures to achieve these objectives.

For this goal, centralized controllers and optimization algorithms including genetic algorithms (GA) [4], hybrid particle swarm optimization (PSO) algorithms [5], and quadratic programming [6] have been proposed in some research publications. These approaches aim to employ economic dispatch to minimize the operational costs of DGs with diverse characteristics. While centralized controllers offer accurate power distribution, they have limitations in terms of flexibility and reliability since they rely on communication lines for data transfer. Moreover, if a central controller unit fails, it can have a significant adverse impact on the overall performance of the system. To overcome these issues, a number of distributed control strategies have been presented to enhance the reliability, flexibility, and economic dispatch of MGs [7]. For example, distributed control schemes based on consensus protocols have been suggested in references [8–12]. These schemes rely solely on the local information of DGs and can improve the reliability of DC MG by leveraging sparse communication channels. Reference [13] presents a decentralized control strategy for achieving cost-efficient performance, where the incremental costs (ICs) are equally distributed among DGs to ensure fair maintenance and minimum total cost. Similarly, in reference [14], economic dispatch is performed in the second layer of the hierarchical control system. By sharing the frequencies of DGs, frequency restoration is achieved, and the ICs are maintained at equal levels. Moreover, in reference [15], a distributed control method has been elaborated that operates on a fixed-time basis, aiming to achieve rapid convergence in solving the economic dispatch problem.

These methods mainly depend on traditional droop control as the primary control mechanism and require a communication network to enable cost optimization in power dispatch. Despite these advancements, there is still a risk of failure due to the presence of communication links.

To address this, numerous enhancements to the droop control strategy have been suggested to improve the performance of a typical DC MG [16, 17]. In [18, 19], adaptive droop approaches are introduced to enhance the accuracy of power sharing and mitigate voltage drops in DC MGs. A different study [20] suggests the implementation of a dynamic droop gain to mitigate power fluctuations. In [21], a dynamic droop control approach is presented to improve the stability of DC MGs. Additionally, [22] proposes a novel converter control method with schedulable variable droop coefficients, addressing low DC voltage issues during drastic power changes and improving variable droop control in multi-terminal DC MGs under heavy loads. On the other hand, [23] introduces a dynamic droop control method optimizing resistance in response to stochastic loads in DC MGs, enhancing current sharing, maintaining stable bus voltage, and effectively addressing random load changes in both common and local loads across distributed sources.

While the classical droop scheme ensures reasonable power distribution among DGs, it does not inherently guarantee the economic operation of DC MGs. Therefore, modifications to the droop control mechanism are necessary for economic operation [24]. To reduce dependence on communication infrastructure, decentralized droop control methods based on cost optimization have been suggested. In reference [24], the classical droop control is adjusted by incorporating offsets formulated from the cost functions of DGs aiming to minimize production costs. These offsets have a non-linear relationship with the generated power. Nonetheless, this scheme is only dependent on one DG as a point of comparison for determining the offsets of other DGs, which may affect the effectiveness of cost-cutting. To address this limitation, a non-linear C_D scheme is introduced in [25], considering economic factors in the control strategy.

In reference [26], linear and non-linear droop methods have been introduced. Ranking DGs by their cost-effectiveness provides the ability to deactivate costly DGs during periods of low demand, thereby further reducing the overall cost. However, relying solely on no-load costs for prioritizing DG dispatch may not always be feasible, especially when DGs with varying cost structures are the same in terms of no-load costs. It is worth noting that the power-sharing commands in [25] and [26] are determined by multiple factors beyond just the DG KW rating. In reference [27], a linear cost-prioritized scheme is employed, regarding multiple factors like production costs, generating capacity, and the quantity of DGs.

An optimal decentralized control approach described in reference [28] is used to achieve cost-effective power distribution by integrating the IC of different DGs in the primary droop control system. On the other hand, in reference [29], the IC is incorporated with decentralized control in the tertiary layer rather than the primary layer. In reference [30], an IC-based droop (IC_D) scheme governs power distribution in hybrid MGs for the AC system in a decentralized manner. Reference [31] uses IC_D control at the primary control level to manage power distribution among a group of MGs. Finally, in [32], mixed-integer conic programming is utilized to compute optimal active and reactive power droop gains. The objective is to minimize costs while adhering to voltage limits, enabling more efficient and economic operation of the MG system.

Several studies including [33–36] have introduced cost-based droop (C_D) schemes to incorporate the operational cost of DGs into the droop control method. In reference [34], for instance, a blended approach that utilizes both F_D and C_D strategies were suggested to enhance the functioning of a DC MG in islanded mode. In reference [35], a frequency-based control method with an embedded cost-based criterion was suggested. Meanwhile, studies such as [34] and [37] demonstrated that by appropriately selecting weighting and scaling factors, the C_D scheme can significantly diminish the production cost (PC) in comparison to the classical droop method.

This paper introduces a novel machine learning (ML)-based hybrid droop strategy for simultaneous minimization of PC and power line loss (PLL) in DC MGs. The approach is designed to optimize MG operation by considering cost and transmission loss factors. As a form of droop scheme, the proposed technique inherits the advantages associated with droop control.

The most challenging aspect of hybrid droop-based strategies lies in determining the importance and effectiveness of each factor, which is measured by the weighting coefficients (WCs). This novel method seeks to optimize these WCs to minimize PC and PLL efficiently. Multiple linear regression is employed to estimate PC and PLL for various WC combinations, and the gradient descent method is utilized to identify optimized WCs leading to the most favourable PC and PLL values. Integrating droop control with ML enhances the accuracy and efficiency of the optimization process, contributing to improved economic and operational performance in DC MGs. To validate the effectiveness of the proposed approach, simulation studies have been conducted under various scenarios. The findings revealed that the suggested droop control strategy generated encouraging outcomes. It is worth mentioning that the DC MG configuration presented in this paper includes both non-dispatchable and dispatchable DGs. Table 1 delineates the contributions of the preceding papers, providing a comparative analysis with the proposed method. To summarize, the main contributions of this paper are outlined as follows:

- **Enhanced performance across load levels**: The proposed method ensures superior performance of the DC MG by optimizing PC and PLL across varying load levels, resulting in improved economic and operational efficiency.
- **Integration of droop control and machine learning**: The paper introduces a novel approach that combines droop control techniques with ML methodologies. This integration utilizes predictive models to estimate PC and PLL, incorporating a gradient descent method to optimize the weights of the controllers. This synergistic approach enhances the accuracy and efficiency of the optimization process.
- **Systematic optimization of WCs**: The assignment of WCs follows a systematic optimization process, eliminating subjectivity or arbitrariness in their selection. This systematic approach enhances the overall performance of the DC MG, ensuring objectivity in the decision-making process.

The paper is arranged in the following way: Section 2 provides an introduction to the arrangement of the DC MG in islanded mode, as well as the coordination objective. Section 3 discusses the IC_D method and the philosophy of a hybrid droop coordination method. Section 4 presents the multiple linear regression. In Section 5, the suggested strategy optimized multiple linear regression based on the droop strategy is introduced. Simulation studies are presented in Section 6 to evaluate the effectiveness of the proposed method. Finally, the paper concludes with Section 7.

TABLE 1 Summary of the literature review conducted for direct current microgrid (DC MG).

Reference No.	Contribution	Objective function	Considering the effect of transmission power loss
[5]	Optimal scheduling model using hybrid PSO	Minimizing operation cost and emission	✗
[4]	Optimization of droop values using GA	Minimizing operation cost	✗
[13]	Droop-based consensus control scheme	Performing economic dispatch	✗
[24]	Autonomous droop scheme	Performing economic dispatch	✗
[25]	Cost-based droop method	Performing economic dispatch	✗
[26]	Linear and non-linear cost-prioritized droop scheme	Performing economic dispatch	✗
[27]	Linear cost-prioritized droop scheme	Performing economic dispatch	✗
[28]	IC in the primary droop	Performing economic dispatch	✗
[29]	IC in the tertiary droop	Performing economic dispatch	✗
[32]	Mixed-integer conic programming	Performing economic dispatch	✗
[36]	Hybrid cost-based droop control	Ensuring economical operation and stability	✗
[34]	Hybrid droop control strategy	Economical operation and flexibility	✗
[37]	Hybrid droop coordination strategy	PC and PLL reduction	✗
Proposed method	Proposed optimized droop control strategy	A machine learning-based approach for minimizing PC and PLL	✓

Abbreviations: GA, genetic algorithms; IC, Incremental cost; PC, production cost; PLL, power line losses; PSO, particle swarm optimization.

2 | DC MG STRUCTURE

This paper examines the structure of an islanded DC MG that includes a photovoltaic (PV) power unit, battery storage, dispatchable DGs, and DC loads (Figure 1).

The PV panel is attached to the DC link via a boost converter, and the battery storage is coupled to the DC link using a bidirectional buck/boost converter [38]. The coordinated control scheme aims to ensure stable operation of the DC MG under varying circumstances of generation and consumption, as well as optimizing the PLL and PC for different power supply and demand ratios.

To achieve these objectives, a set of fundamental principles were implemented, such as giving distributed energy resources (DERs) with the lowest power generation cost a greater emphasis in power distribution to reduce PC, and assigning a more significant position in power distribution to DERs located electrically closer to the DC bus to reduce PLL. Additionally, the fundamental concept of the various droop control methods

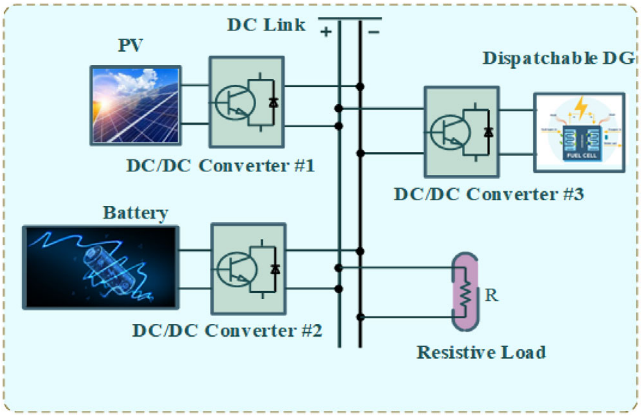

FIGURE 1 A single-line representation of the proposed direct current (DC) microgrid (MG) configuration.

such as classical, hybrid, etc., and optimized multiple linear regression strategy have been discussed briefly in the following section.

3 | EVALUATING THE PERFORMANCE OF DROOP CONTROL METHODS FOR MGS

This section will undertake a comprehensive examination of various droop control methods.

3.1 | Classical droop control method

The classical droop control is employed for power sharing among DGs in a DC MG. In this method, the power distribution of DGs is based on their generation capability [39]. The droop control technique utilizes local parameters for power distribution, thereby eliminating the need for a communication link [39]. The droop method equations for MGs can be described simply in the following manner, according to reference [28]:

$$V_{R,i} = V_{\max} - k_i P_i \tag{1}$$

$$k_i = \frac{V_{\max} - V_{\min}}{P_{\max i}}. \tag{2}$$

In the above equations, $V_{\mathrm{R,i}}$ represents the bus voltage, P_i denotes the output power of the i^{th} DG, and k_i signifies the droop coefficient associated with that DG. By assuming that the terminal voltages of all DGs are equal and using Equation (1), the equation provided can be derived for an MG consisting of n DGs. [27, 30, 31]:

$$k_1 P_1 = k_2 P_2 = \cdots = k_n\, P_n \tag{3}$$

3.2 | IC_D technique

In the classical droop control technique, DGs with higher nominal power are given higher priority. However, if the aim is to reduce operational costs, the IC_D method is employed to allocate power between various DGs. In this approach, DGs with lower operating costs are given higher priority in supplying the load. As a result, it is possible to reduce the PC without the need for any communication infrastructure. The following equation is utilized to calculate the PC of the DC MG with n number of inputs [37]:

$$PC = \sum_{i=1}^{n} C_i\,(P_i) \tag{4}$$

where $\mathrm{C_i(P_i)}$ is incur generation costs of the i^{th} DG. The optimal power distribution among the DGs is achieved by equating their IC functions, which are the derivatives of their respective cost functions. This helps minimize the PC without requiring any communication infrastructure. This approach is formulated as follows [37]:

$$V_{R,i} = V_{\max} - Q\left(IC_{P,i}\,(P_i)\right) \tag{5}$$

$$Q = \frac{V_{\max} - V_{\min}}{\max\left\{\left(IC_1\,(P_{1\,\max})\right), \left(IC_2\,(P_{2\,\max})\right), \ldots, \left(IC_i\,(P_{i\,\max})\right)\right\}} \tag{6}$$

In the method discussed, the droop slope is denoted as Q, while $IC_{P,i}(P_i)$ represents the cost function's derivative. Equation (5) shows that the reference voltage of the i^{th} DG depends on its generation cost. This means that each DG is given priority based on its cost-to-value ratio relative to the most expensive unit. Equation (7) ensures economic validity in the mentioned method by maintaining voltage equality among the DGs [37].

$$IC_{P,1}\,(P_1) = IC_{P,2}\,(P_2) = \cdots = IC_{P,i}\,(P_i) \tag{7}$$

3.3 | Loss-based droop method

The loss-based droop method is defined through a formulated quadratic power loss function for each dispatchable DG. This method aims to optimize power-sharing in an MG while minimizing transmission line power losses. Equation (8) defines this function, where $P_{Loss,i}$ denotes the transmission line power loss and $\mathrm{I_i}$ represents the injecting current of the i^{th} DG, with $\mathrm{R_{L,i}}$ denoting the resistance of the line connecting the load bus to the i^{th} DG [37].

$$P_{Loss,i} = R_{L,i}\, I_i^2 \tag{8}$$

The cumulative power loss of the transmission line in the MG is represented by Equation (9) [37].

$$TL = \sum_{i=1}^{n} P_{Loss,i}\,(I_i) \tag{9}$$

To determine the reference voltage for power sharing, Equations (10) and (11) are employed, where N represents a constant obtained from (11) signifying the slope of the loss-based power sharing, and $P'_{\mathrm{Loss,i}}$ denotes the derivative of the power loss function:

$$V_{\mathrm{ref,i}} = V_{\max} - N\left(P'_{\mathrm{Loss,i}}\left(I_i\right)\right) \tag{10}$$

$$N = \frac{V_{\max} - V_{\min}}{\max\left\{\left(P'_{\mathrm{Loss,1}}\right), \left(P'_{\mathrm{Loss,2}}\right), \ldots, \left(P'_{\mathrm{Loss,i}}\right)\right\}} \tag{11}$$

From Equation (10), it is evident that $V_{\mathrm{ref,i}}$ is correlated with the power loss of the i^{th} DG. Consequently, each DG is prioritized based on the ratio of its power loss function derivative to the maximum power loss function derivative of units at nominal value [37].

Under the assumption of terminal voltage equality for DGs in (10), power-sharing in the presence of power loss, ensuring minimal power loss, is consistently upheld by (12) [37]. Unlike the IC_D method where optimization is demonstrated by the equality of cost function derivatives, our proposed loss-based droop method achieves optimization through the equality of power loss function derivatives of units.

$$P'_{\mathrm{Loss,1}}\left(I_1\right) = P'_{\mathrm{Loss,2}}\left(I_2\right) = \cdots = P'_{\mathrm{Loss,n}}\left(I_n\right) \tag{12}$$

3.4 | Hybrid droop coordination strategy

As mentioned in the preceding subsection, the IC_D method allocates power among DGs by prioritizing each DG based on its economic criterion. However, in the hybrid droop technique, it is possible to consider both PC and PLL simultaneously. The hybrid method involves finding a balance between the IC_D method and the L_D method, where both methods contribute to power distribution according to their respective WCs.

In scenarios where minimizing power loss is of higher importance, it can be advantageous to allocate power between units based on the loss criterion. This implies that units connected through lower-resistance lines are prioritized in power distribution to meet the load demand.

Following the presentation of the IC_D and L_D methods in [36], a hybrid droop coordination approach that incorporates both power loss and cost function has been introduced. The method's effectiveness is demonstrated through Equations (13) and (14).

$$V_{\mathrm{R,i}} = V_{\max} - \mathrm{H_i} \tag{13}$$

$$H_{\mathrm{i}} = \left(V_{\max} - V_{\min}\right)\left(\mathrm{WC_1 a} + \mathrm{WC_2 b}\right) \tag{14}$$

$$a = \frac{IC_{P,i}\left(P_i\right)}{max\left\{\left(IC_1\left(P_{1\,\max}\right)\right), \left(IC_2\left(P_{2\,\max}\right)\right), \ldots, \left(IC_i\left(P_{i\,\max}\right)\right)\right\}}$$

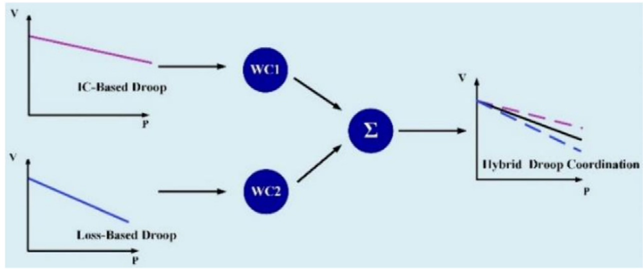

FIGURE 2 Hybrid droop method: Incorporating IC-based droop (IC_D) and loss-based droop (L_D) approaches with weighting coefficients (WCs).

$$\mathrm{b} = \frac{P'_{\mathrm{Loss,i}}}{\max\left\{\left(P'_{\mathrm{Loss,1}}\right), \left(P'_{\mathrm{Loss,2}}\right), \ldots, \left(P'_{\mathrm{Loss,i}}\right)\right\}}$$

Similar to Equation (14), the constant value H_i corresponds to the slope of the hybrid droop in Equation (15). The weight factors for cost and loss are represented by $\mathrm{WC_1}$ and $\mathrm{WC_2}$, respectively. As mitigating costs and power losses both are important, the WCs are chosen by the operator in a way that $\mathrm{WC_1}$ and $\mathrm{WC_2}$ add up to one. Equation (15) ensures the consistent effectiveness of the hybrid droop coordination method by maintaining the equality of the bus voltage of each DG [36].

$$H_1 = H_2 = \cdots = H_n \tag{15}$$

Figure 2 illustrates the merging of the IC_D plus L_D methods through the utilization of WCs. As both methods are incorporated into the hybrid droop coordination approach based on the WCs, they contribute to the method's effectiveness.

4 | LINEAR REGRESSION

Linear regression is a statistical method that employs a linear equation to model the correlation between an affiliate variable Y and one or more autonomous variables X. Its primary goal is to determine the most suitable line of best fit that can predict the value of Y with precision based on a given value of X. When there are several independent variables, the linear regression formula expands to Equation (16):

$$Y = \beta_0 + \beta_1 X_1 + \beta_2 X_2 + \beta_k X_k + \varepsilon. \tag{16}$$

The equation for multiple linear regression involves k independent variables, denoted as X_1, X_2, …, X_k and their corresponding coefficients, represented by β_1, β_2, …, β_k. The goal remains to determine the ideal coefficients that minimize the sum of squared errors between the predicted and observed values of Y. The MSE gauges the mean squared difference between the predicted values and the real values in the dataset. It can be calculated as follows (17):

$$\mathrm{MSE} = \frac{1}{n}\sum_{i=1}^{n}\left(y_i - \hat{y}_i\right)^2, \tag{17}$$

where n is the number of data points, y_i is the actual value of the affiliate variable for the i^{th} data point, and $\hat{y}_i$ is the forecasted value of the affiliate variable for the i^{th} data point.

In simpler terms, the MSE is the average of the squared differences between the predicted and actual values of the dependent variable. A lower MSE indicates that the model is fitting the data better. Furthermore, R-squared is a different metric employed to evaluate the goodness of fit of a linear regression model. The formula for R-squared is (18):

$$R^2 = 1 - (SSE/SST), \tag{18}$$

where SSE is the sum of squared errors and SST is the total sum of squares. It should be noted that SST measures the total variation in the dependent variable, while SSE measures the unexplained variation in the dependent variable.

5 | PROPOSED METHOD: OPTIMIZED HYBRID DROOP COORDINATION STRATEGY USING LINEAR REGRESSION

The hybrid droop strategy has emerged as a promising approach to enhance the efficiency of DC MGs by combining the benefits of both IC_D and L_D techniques. However, the effectiveness of this strategy heavily relies on the appropriate selection of WCs governing the contribution of each droop strategy. In the existing literature, the determination of WCs has often been subjective, relying on arbitrary choices or empirical observations. This lack of systematic optimization limits the ability to fully exploit the potential benefits of the hybrid droop strategy. Given the significance of the aforementioned challenge, an ML-based method is suggested in this study to address the existing concerns. The suggested method utilizes multiple linear regression and gradient descent techniques to optimize the WCs and enhance the performance of the hybrid droop strategy. By modelling the relationship between WCs, PC, PLL, and loads, the suggested method aim to find the optimal WCs and tune them to optimize the hybrid droop strategy. The proposed method involves two primary steps: firstly, training the linear regression model, and secondly, determining the optimized WCs using the gradient descent algorithm. Subsequent sections will elaborate on each of these steps in detail.

5.1 | Linear regression model training

Using multiple linear regression, the WCs and loads are considered independent variables, while the dependent variables are PCs and PLLs. A multiple linear regression model is trained using simulation data that includes various combinations of WCs, loads, PCs, and PLLs. This allows the model to learn the underlying patterns and relationships between these variables. Once the multiple linear regression model is trained, it can be used to predict the values of PC and PLL for a given set of WCs and loads. This prediction capability enables us to optimize the hybrid droop strategy by finding the optimal combination of WCs that minimizes PC and PLL, leading to improved performance. Here's a breakdown of the tuning process:

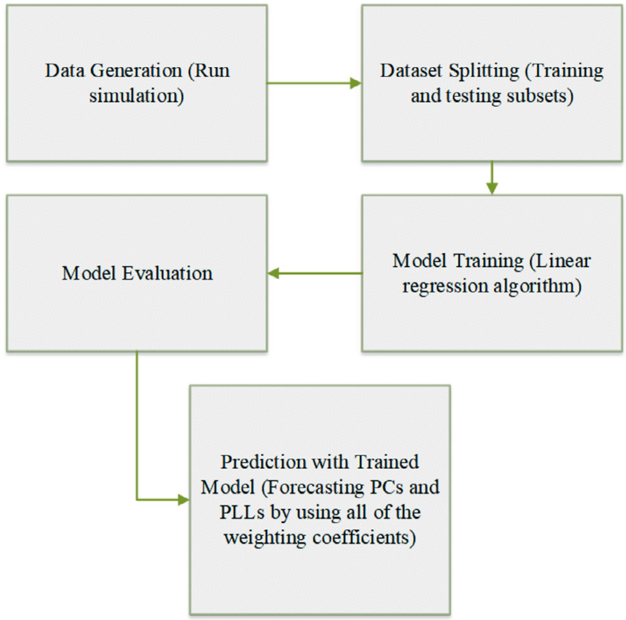

FIGURE 3 Linear regression tuning process flowchart. PC, production cost; PLL, power line loss.

1. Data generation: We simulate the strategy for a specified number of iterations to generate a dataset of PC and PLL values for each set of WCs and loads.
2. Dataset splitting: The generated dataset is split into training and testing subsets to facilitate model training and evaluation.
3. Model training: We train a linear regression model using the training subset to learn the relationship between the WCs, loads, PC, and PLL values.
4. Model evaluation: The accuracy of the trained linear regression model is evaluated using the testing subset based on criteria such as MSE and R-squared (R^2).
5. Prediction with trained model: Once the linear regression model is trained using the dataset, it becomes capable of predicting the PC and PLL values for a large number of random combinations of WCs and loads. These predictions are based on the learned relationships between the independent variables (WCs and loads) and the dependent variables (PC and PLL).

Furthermore, the multiple linear regression model can also be utilized to predict DC MG quantities such as PC and PLL. This information can provide valuable insights into the overall system behaviour and assist in decision-making processes. Figure 3 illustrates the steps involved in the gradient descent process.

5.2 | Optimization with gradient descent

After obtaining predictions for PC and PLL, the next step is to optimize these values to identify the most suitable WCs for the hybrid droop coordination approach. This is where the gradient descent algorithm comes into play.

The suggested method incorporates the use of the gradient descent algorithm to fine-tune the WCs and minimize the values of PC and PLL. This choice is rooted in the algorithm's demonstrated efficacy in optimizing high-dimensional models, making it well-suited for this paper's specific problem. Its simplicity and versatility enhance the efficiency of our optimization process by seamlessly integrating with the multiple linear regression model. To fine-tune the WCs and minimize the values of PC and PLL, the multiple linear regression model generates multiple results and predictions based on different combinations of WCs and loads. The gradient descent algorithm takes the predictions from the multiple linear regression model and iteratively adjusts the WCs to minimize the values of PC and PLL. By iteratively updating the weighting factors in the direction that reduces the error, the algorithm progressively converges toward the optimal values.

The optimization with gradient descent process involves the following steps:

1. Initialization: Start with an initial guess for the WCs. This could be random or based on prior knowledge.
2. Calculate gradient: Compute the gradient of the cost or loss function with respect to each WC. The gradient indicates the direction of the steepest increase of the function.
3. Update WCs: Adjust the WCs in the direction opposite to the gradient to minimize the cost or loss function. This adjustment is proportional to the gradient and a predefined learning rate, which determines the size of the steps taken in each iteration.
4. Iterate: Repeat steps 2 and 3 until convergence criteria are met. Convergence is typically achieved when the changes in the WCs become very small or when the cost or loss function reaches a minimum.
5. Iterative optimization: During each iteration of gradient descent, the algorithm adjusts the WCs to minimize the predicted values of PC and PLL. By iteratively updating the WCs in the direction that reduces the error between the predicted and actual values, the algorithm gradually converges toward the optimal values of the WCs.
6. Identification of suitable WCs: Once the gradient descent optimization process converges, the optimized PC and PLL values are utilized to identify the most suitable WCs for the hybrid droop coordination approach. These WCs represent the optimal configuration that minimizes production cost and power line losses, thus enhancing the performance of the hybrid droop strategy.

Figure 4 illustrates the steps involved in the gradient descent process.

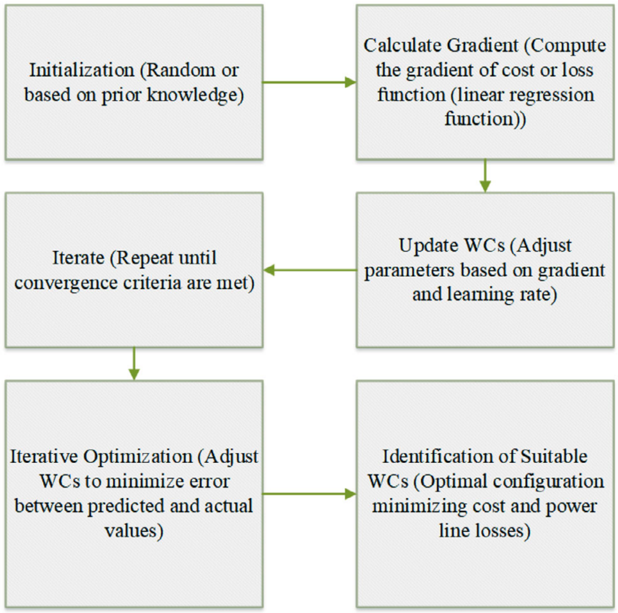

FIGURE 4 Gradient descent-based tuning algorithm for hybrid droop coordination optimization. WC, weighting coefficient.

Through this iterative optimization process, the suggested method can effectively determine the weighting factors that offer the best performance for the hybrid droop strategy. The combination of multiple linear regression and the gradient descent algorithm allows for a systematic approach to finding and fine-tuning the WCs, overcoming the limitations of subjective or empirical methods used in previous studies.

6 | SIMULATION RESULTS AND ANALYSIS

To implement the proposed droop control method on our DC MG (see Figure 1), Matlab/Simulink has been used. The simulation parameters have also been provided in Tables A1 and A2 in the Appendix. Notably, the quadratic cost functions are chosen based on references [25], [27], and [28], with the cost function coefficients (ai1, ai2, and ai3) of each DGs scaled identically to those in references [25], [27], and [28].

6.1 | Simulation parameters and assumptions

To demonstrate the entire process and evaluate the system's performance in the worst-case scenario, different transmission line resistances are taken into account. For instance, the proposed method's power distribution performance is compared with the hybrid droop coordination method and the classical one. Moreover, the dispatchable DGs are considered to be identical in nominal power. Additionally, the MG under study includes five resistance loads. The following parameters are essential for understanding the system's behaviour:

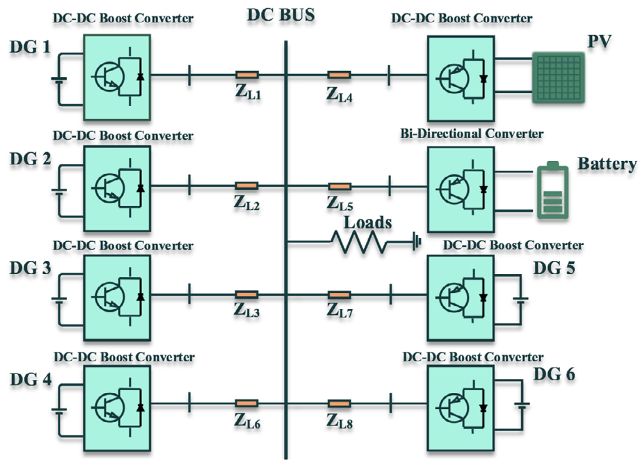

FIGURE 5 Schematic of direct current (DC) microgrid (MG) in the case study.

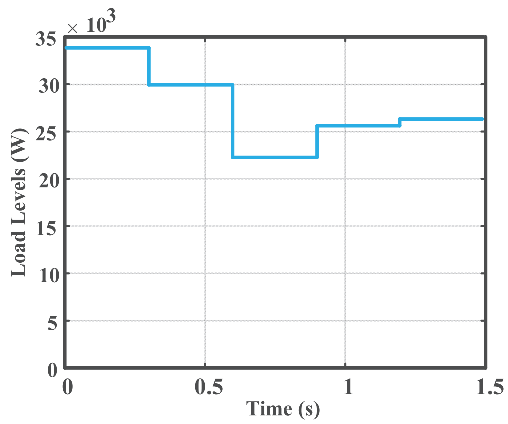

FIGURE 6 Different load levels.

- -DC link voltage: Set to 100 volts, with a permissible fluctuation range between 95 and 105 V.
- -Solar power generation: Operates under MPPT (maximum power point tracking) conditions utilizing fuzzy logic, consistently producing 1.6 kW of power.
- -Converters: The boost converter parameters, including controller coefficients, inductor and capacitor values, input voltage, rated power, and switching frequency of 50 kHz, are specified.

These parameters collectively contribute to the comprehensive evaluation of the system's performance and provide insights into its behaviour under various operating conditions.

6.2 | Case study

The DC MG comprising six DGs with the same nominal power is depicted in Figure 5. Moreover, Figure 6 illustrates the load levels. Notably, a comparative study has also been considered to evaluate the performance of different methods.

Figure 7a–e illustrates the power waveforms of DERs. Figure 7f illustrates the power waveforms of DERs using the suggested method, incorporating tuned WCs, under different load levels. Initially, the assessment of the proposed approach is based on the MSE and R^2 metrics. These metrics are used to determine the accuracy of predictions. Incorporating the proposed strategy yields: MSE = 37, R^2 = 0.98. Furthermore, Table 2 presents the actual and predicted values for PC and PLL, indicating that the suggested method's accuracy is valid. Considering the following scenarios, the performance of the optimized droop technique proposed here is also evaluated with classical droop and hybrid one.

a) *Scenario 1*: $0 < t < t_1$

At the beginning, there is a load level of 35.5 kW that needs to be met with the power generated by DERs for loads 2, 3, and 4. In this case, the WCs for forecasting the optimum PC and PLL of the suggested method are equal to:

WC1 = 0.0, WC2 = 1, WC3 = 0.85, WC4 = 0.15, WC5 = 0.35, WC6 = 0.65, WC7 = 0.88, WC8 = 0.12, WC9 = 0.96, WC10 = 0.04, WC11 = 0.18, WC12 = 0.82.

b) *Scenario 2*: $t_1 < t < t_2$

when $t = t_1$, the power demand for load 4 becomes zero, leading to a reduction in power consumption from 35.5 to 30 kW. As a result, the suggested method employs the following WCs:

WC1 = 0.02, WC2 = 0.98, WC3 = 0.58, WC4 = 0.42, WC5 = 0.57, WC6 = 0.43, WC7 = 0.91, WC8 = 0.09, WC9 = 0.31, WC10 = 0.69, WC11 = 0.14, WC12 = 0.86

c) *Scenario 3*: $t_2 < t < t_3$

At time $t = t_2$, load 1′s demand must be met, causing load 3′s power demand to drop to zero (30 to 22.5 kW). The method adapts WCs to optimize PC and PLL for supplying loads 1 and 2.

WC1 = 0.01, WC2 = 0.99, WC3 = 0.49, WC4 = 0.51, WC5 = 0.78, WC6 = 0.22, WC7 = 0.81, WC8 = 0.19, WC9 = 0.48, WC10 = 0.52, WC11 = 0.14, and WC12 = 0.86.

d) *Scenario 4*: $t_3 < t < t_4$

At $t = t_3$, the power demand for load 5 also needs to be fulfilled, leading to an increase in power consumption from 22.5 to 26 kW. As a result, to meet the energy demands of loads 1, 2, 3, and 5, the DERs must produce electricity. To achieve the optimal PC and PLL in this situation, the suggested method utilizes the following WCs:

WC1 = 0.13, WC2 = 0.87, WC3 = 0.67, WC4 = 0.33, WC5 = 0.33, WC6 = 0.67, WC7 = 0.8, WC8 = 0.2, WC9 = 0.68, WC10 = 0.32, WC11 = 0.64, and WC12 = 0.36.

e) *Scenario 5*: $t_4 < t < t_5$

At $t = t_4$, the power required for load 1 drops to zero, which causes a decrease in power consumption from 26 to 27 kW.

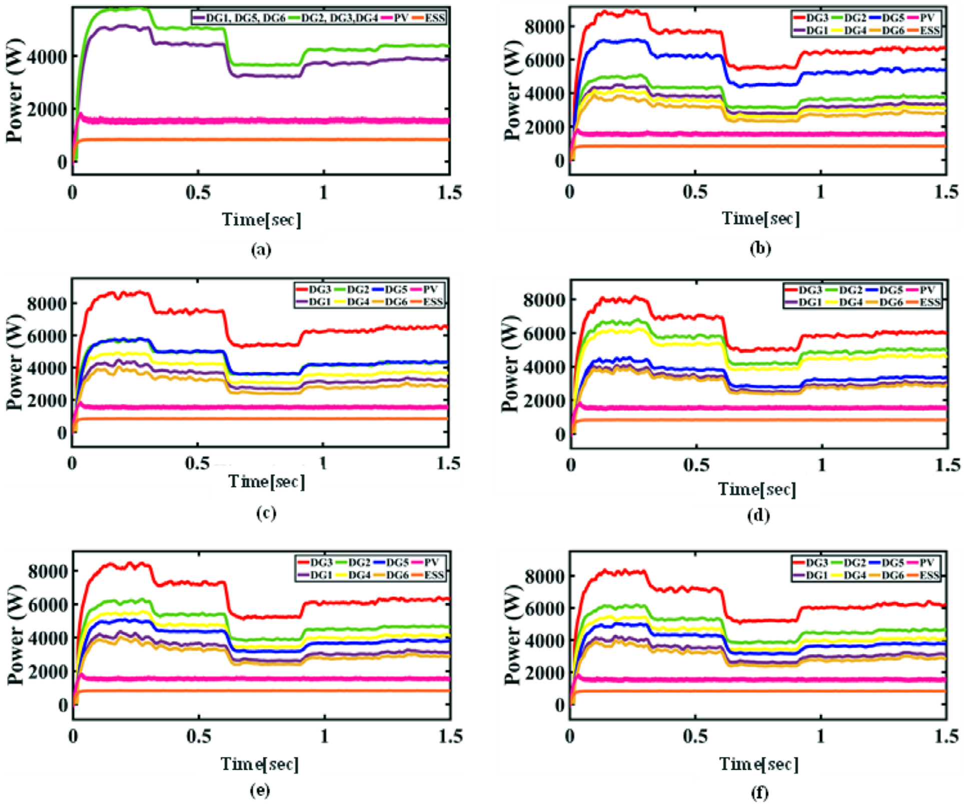

FIGURE 7 Power waveforms of different distributed energy resources (DERs): (a) Classical, (b) IC-based droop (IC_D), (c) hybrid in first status, (d) hybrid in third status, (e) hybrid second status, and (f) proposed method.

TABLE 2 A comparison of direct current microgrid's (DCMG)'s actual values with its predicted values.

	WCs													Predicted values		Actual values		Error	
	WC_1	WC_2	WC_3	WC_4	WC_5	WC_6	WC_7	WC_8	WC_9	WC_{10}	WC_{11}	WC_{12}	Load	PC	PLL	PC	PLL	PC	PLL
1	0.15	0.85	0.85	0.15	0.35	0.65	0.1	0.9	0.85	0.15	0.75	0.25	29.955	82.58	222.23	81.1	214.38	1.8%	3.66%
2	0.1	0.9	0.75	0.25	0.25	0.75	0.4	0.6	0.65	0.35	0.2	0.8	29.9	80.24	207.568	85.4	202	6%	2.75%
3	0.8	0.2	0.65	0.35	0.5	0.5	0.9	0.1	0.15	0.85	0.25	0.75	29.732	80.336	206.55	78.62	207.2	2.18%	0.31%
4	0.7	0.3	0.25	0.75	0.55	0.45	0.45	0.55	0.4	0.6	0.8	0.2	24.984	57.816	145.613	55.37	136.7	4.41%	6.52%
5	0.1	0.9	0.2	0.8	0.45	0.55	0.5	0.5	0.85	0.15	0.75	0.25	24.88	51.05	142.315	53	144.1	3.67%	1.23%
6	0.25	0.75	0.9	0.1	0.35	0.65	0.85	0.15	0.6	0.4	0.25	0.75	24.93	47.904	133.271	51.6	140.5	7.16%	5.14%
7	0.15	0.85	0.85	0.15	0.35	0.65	0.65	0.35	0.55	0.45	0.45	0.55	24.83	50.187	133.382	52	138.25	3.48%	3.52%
8	0.1	0.9	0.2	0.8	0.45	0.55	0.5	0.5	0.85	0.15	0.75	0.25	34.245	103.58	280.672	104	287.9	0.4%	2.51%
9	0.25	0.75	0.4	0.6	0.55	0.45	0.55	0.45	0.3	0.7	0.7	0.3	34.223	107.714	277.054	106.8	271.8	0.8%	1.93%
10	0.6	0.4	0.3	0.7	0.75	0.25	0	1	1	0	0.1	0.9	34.64	109.049	290.809	109.45	295	0.3%	1.42%

Abbreviations: PC, production cost; PLL, power line losses; WC, weighting coefficient.

Therefore, the suggested method uses the set of WCs listed below to optimize PC and PLL:

WC1 = 0.25, WC2 = 0.75, WC3 = 0.73, WC4 = 0.27, WC5 = 0.62, WC6 = 0.38, WC7 = 0.98, WC8 = 0.02, WC9 = 0.8, WC10 = 0.2, WC11 = 0.18, and WC12 = 0.82.

The hybrid droop coordination method comprises three distinct statuses, as follows:

- First status: WC1 = 0.7, WC2 = 0.3, WC3 = 0.7, WC4 = 0.3, WC5 = 0.7, WC6 = 0.3, WC7 = 0.7, WC8 = 0.3, WC9 = 0.7, WC10 = 0.3, WC11 = 0.7, WC12 = 0.3
- Second status: WC1 = 0.5, WC2 = 0.5, WC3 = 0.5, WC4 = 0.5, WC5 = 0.5, WC6 = 0.5, WC7 = 0.5, WC8 = 0.5, WC9 = 0.5, WC10 = 0.5, WC11 = 0.5, WC12 = 0.5

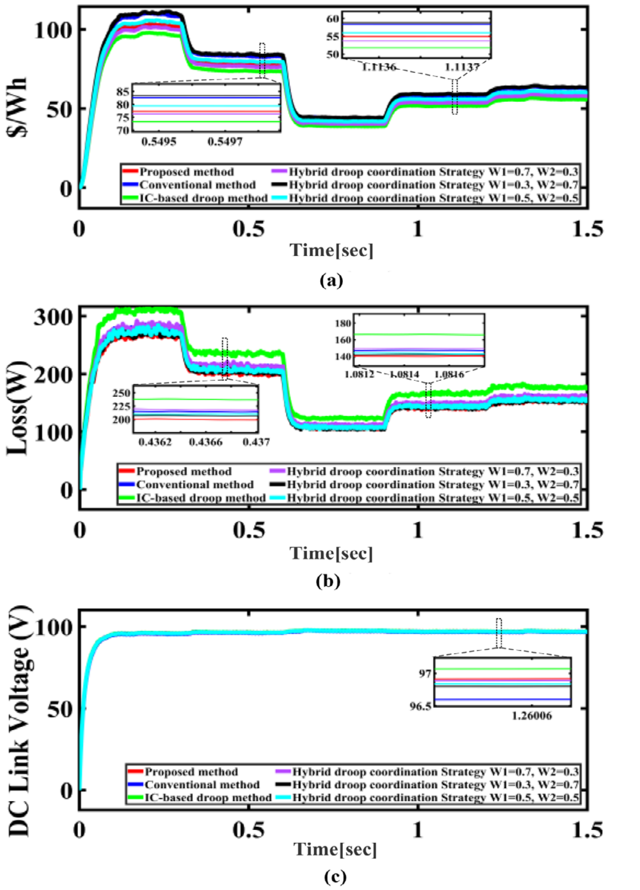

FIGURE 8 Comparative analysis of the proposed method versus classical, IC_D method, hybrid method: (a) production cost (PC); (b) power line losses (PLL); (c) direct current (DC) link voltage.

- Third status: WC1 = 0.3, WC2 = 0.7, WC3 = 0.3, WC4 = 0.7, WC5 = 0.3, WC6 = 0.7, WC7 = 0.3, WC8 = 0.7, WC9 = 0.3, WC10 = 0.7, WC11 = 0.3, WC12 = 0.7

As it turns out, an AC-based droop control scheme can be deduced using the hybrid scheme. When the WCs in the hybrid method are set to WC1 = 1 and WC2 = 0, the performance of this method becomes equivalent to that of the IC_D method.

6.3 | Comparative study

A comparison is made between the proposed method versus classical and hybrid methods and the obtained results are depicted in Figure 8a–c. The figure demonstrates that the method elaborated here exhibits improvements regarding PLL and PC compared to other aforesaid techniques.

In the method presented here, the WCs are predicted using the multiple linear regression algorithm in a way that leads to the optimal PC and PLL. This strategy yields reduced PC and PLL values, as shown in Figure 9 when compared to both the hybrid droop coordination and classical methods. The classical method is used as a benchmark for comparison. The reduction in PC and PLL is represented by positive percentages, while any increase is indicated by negative percentages.

Another superiority of the suggested method is the tracking of PC and PLL with the accurate selection of WCs. The DC link voltage in the suggested method is evaluated with various scenarios of the conventional and hybrid droop methods in Figure 8c. The suggested approach demonstrates a smaller reduction in the DC link voltage in comparison to the classical and hybrid droop methods.

6.4 | Sensitivity analysis

In this subsection, we conducted a sensitivity analysis of the eigenvalues to assess the impact of the droop coefficients on system stability. To commence, Figure 10 illustrates an averaged equivalent model of the droop-controlled DC MG with n DG, incorporating the dynamic elements of the DG converters. For the sake of simplicity, we examined a two-DG system, as depicted in Figure 11.

With the state equations in place, small-signal modelling of the DC MG can be achieved. By using perturbation and linearization of the model described in Equations (19)–(22), the small-signal model can be expressed with the following general state-space form:

$$L_j \frac{di_{L_j}}{dt} = V_{in_j} u_j - v_{c_j}, \tag{19}$$

$$C_j \frac{dv_{c_j}}{dt} = i_{L_j} - i_{o_j}, \tag{20}$$

$$L_{e_j} \frac{di_{o_j}}{dt} = v_{c_j} - i_{o_j}\left(R_{d_j} + R_{L_j}\right) - v_{dcbus}, \tag{21}$$

$$C_{dc-bus} \frac{dv_{dcbus}}{dt} = \sum_{j=1}^{2} i_{o_j} - \frac{v_{dcbus}}{R}. \tag{22}$$

The state equation describing the model is given as follows:

$$\dot{\hat{x}} = A_{sys}\hat{x} - B_{sys}\hat{u} \tag{23}$$

where $\hat{x} = [\hat{x}_1 \hat{i}_{L_1} \hat{v}_{c_1}\ \hat{i}_{o_1}\ \hat{x}_2\ \hat{i}_{L_2}\ \hat{v}_{c_2}\ \hat{i}_{o_2}\ \hat{v}_{dcbus}]^T$ are state variables, with $\hat{x}_1$ and $\hat{x}_2$ being the integration variable of the output voltage of DGs. The overall A_{sys} in Equation (23) can be derived as:

$$A_{sys} = \begin{bmatrix} 0 & 0 & a_{13} & a_{14} & 0 & 0 & 0 & 0 & 0 \\ a_{21} & 0 & a_{23} & a_{24} & 0 & 0 & 0 & 0 & 0 \\ 0 & a_{32} & 0 & a_{34} & 0 & 0 & 0 & 0 & 0 \\ 0 & 0 & a_{43} & a_{44} & 0 & 0 & 0 & 0 & a_{49} \\ 0 & 0 & 0 & 0 & 0 & 0 & a_{57} & a_{58} & 0 \\ 0 & 0 & 0 & 0 & a_{65} & 0 & a_{67} & a_{68} & 0 \\ 0 & 0 & 0 & 0 & 0 & a_{76} & 0 & a_{78} & 0 \\ 0 & 0 & 0 & 0 & 0 & 0 & a_{87} & a_{88} & a_{89} \\ 0 & 0 & 0 & a_{94} & 0 & 0 & 0 & a_{98} & a_{99} \end{bmatrix}.$$

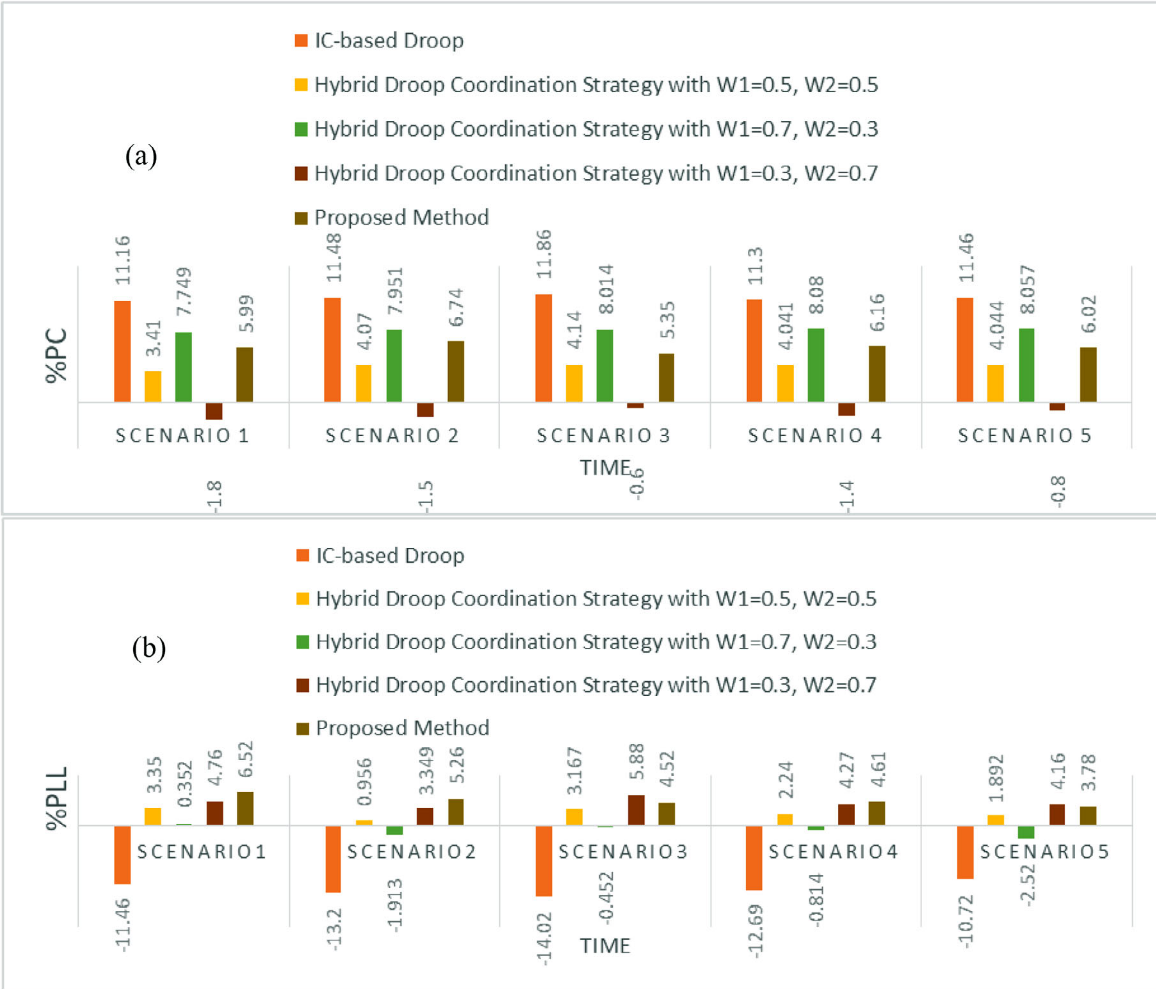

FIGURE 9 Performance evaluation of proposed method versus classical and hybrid droop coordination methods: (a) production cost (PC); (b) power line losses (PLL).

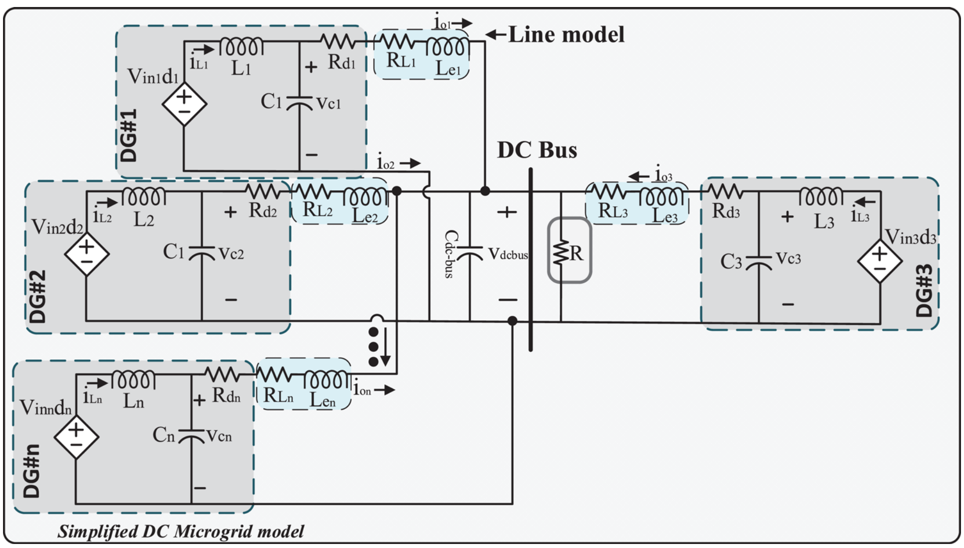

FIGURE 10 Averaged model of the droop-controlled direct current (DC) microgrid (MG).

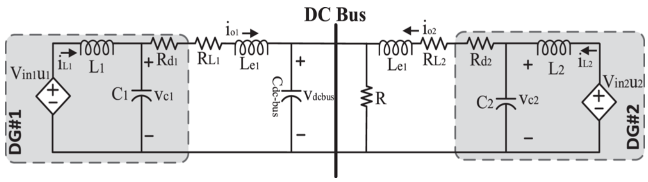

FIGURE 11 Averaged model of the droop-controlled direct current (DC) microgrid (MG) with two DGs.

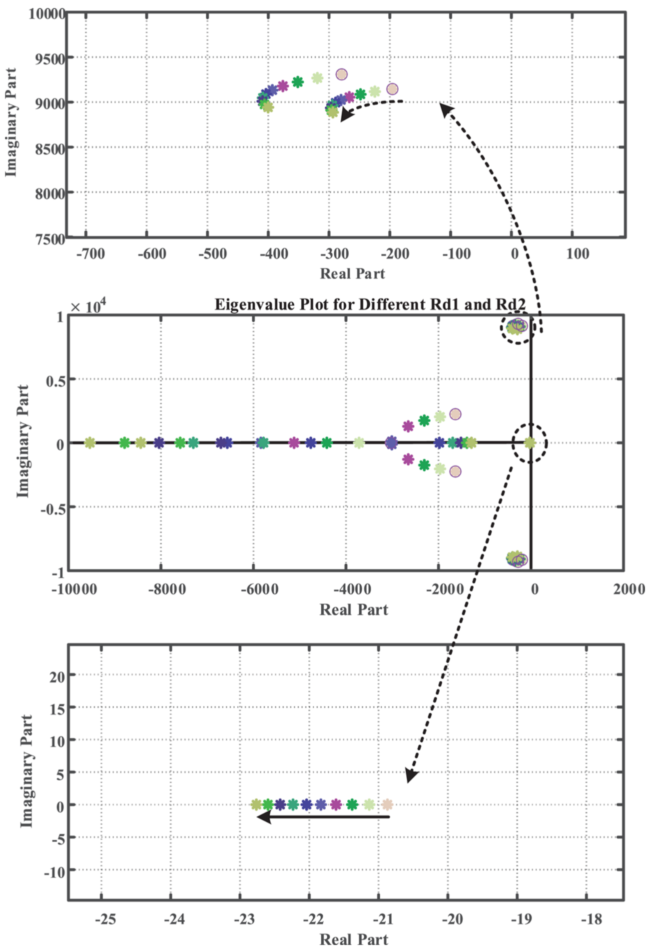

FIGURE 12 The movement of eigenvalues for the two-DG system with varying droop resistance.

The parameters in the above matrix are given in Appendix. With the system matrix A_{sys} established, eigenvalue analysis can be performed in the presence of controllers and droop coefficients. We investigated the impact of droop coefficients on the stability of the entire system by varying the values of droop resistances ($0.33 \leq R_{d_1} \leq 1$, $0.33 \leq R_{d_2} \leq 1$), and the obtained results are illustrated in Figure 12. It is worth noting that the "*participation factor method*" can be employed to precisely determine the contribution or influence of a specific state variable to a specific mode for various system design requirements such as droop resistance. In our system, as depicted in Figure 11, the real part of eigenvalues, especially those in close proximity to the origin, shifts from right to left as the droop coefficient values increase, which is beneficial to the system's stability.

7 | CONCLUSION

This paper presented an ML-based optimized droop control method for DC MGs, aiming to minimize the PC and PLL. By introducing a systematic approach that harnesses the benefits of AI, accurate predictions of PLL and PC were made possible. Leveraging the gradient descent method, the suggested technique independently optimized PC and PLL for each scenario, eliminating the need for arbitrary adjustments of WCs as required in traditional hybrid droop coordination strategies. The comparative analysis confirmed the superiority of the droop scheme presented here over the traditional and hybrid approaches, showcasing its effectiveness in enhancing the performance of DC MGs regarding operating cost optimization and transmission loss reduction. Thus, PC and PLL in the proposed method, considering the conventional method as a benchmark in different scenarios, have been improved by about 6% and 4.5%, respectively. Furthermore, the decentralized nature of the suggested coordination technique eliminated the need for costly infrastructure, offered greater reliability, and reduced complexity when compared to communication link-based strategies. Overall, this research contributed to the advancement of droop control in DC MGs, demonstrating the potential of ML and optimization techniques for achieving significant improvements in economic and operational efficiency. In future work, the proposed ML-based optimized droop control method for DC MGs could be extended and adapted for application in AC MGs.

NOMENCLATURE

ML	Machine learning
DC	Direct current
DG	Distributed generation
AI	Artificial intelligence
MSE	Mean squared error
MG	Microgrid
RES	Renewable energy source
MPPT	Maximum power point tracking
IC	Incremental cost
PC	Production cost
PLL	Power line loss
DER	Distributed energy resources
PV	Photovoltaic
SSE	Sum of squared errors
SST	Total sum of squares
TSS	Total sum of squares
WC	Weighting coefficient
C_D	Cost-based droop
IC_D	IC-based droop
L_D	Loss-based droop
F_D	Flexibility-based droop

AUTHOR CONTRIBUTIONS

Younes Saeidinia: Conceptualization; formal analysis; investigation; methodology; software; validation; visualization; writing—original draft. **Mohammadreza Arabshahi**: Conceptualization; formal analysis; investigation; methodology; software; validation; visualization; writing—original draft. **Mohammad Aminirad**: Conceptualization; formal analysis; investigation; methodology; software; validation; visualization; writing—original draft. **Miadreza Shafie-khah**: Conceptualization; formal analysis; resources; supervision; investigation; validation; writing—review and editing.

CONFLICT OF INTEREST STATEMENT

The authors declare no conflicts of interest.

DATA AVAILABILITY STATEMENT

Research data are not shared.

ORCID

Younes Saeidinia https://orcid.org/0009-0001-3903-4860
Mohammadreza Arabshahi https://orcid.org/0000-0003-3157-2805

REFERENCES

1. Hatahet, W., Marei, M.I., Mokhtar, M.: Adaptive controllers for grid-connected DC microgrids. Int. J. Elect. Power Energy Syst. 130, 106917 (2021)
2. Barik, A.K., Tripathy, D., Das, D.C., Sahoo, S.C.: Optimal load-frequency regulation of demand response supported isolated hybrid microgrid using fuzzy PD+I controller. In: Intelligent Techniques and Applications in Science and Technology: Proceedings of the First International Conference on Innovations in Modern Science and Technology, pp. 798–806. Springer International Publishing, Berlin (2020)
3. Díaz, N.L., Vasquez, J.C., Guerrero, J.M.: A communication-less distributed control architecture for islanded microgrids with renewable generation and storage. IEEE Trans. Power Electron. 33(3), 1922–1939 (2017)
4. Li, C., De Bosio, F., Chen, F., Chaudhary, S.K., Vasquez, J.C., Guerrero, J.M.: Economic dispatch for operating cost minimization under real-time pricing in droop-controlled DC microgrid. IEEE J. Emerg. Sel. Top. Power Electron. 5(1), 587–595 (2016)
5. Deng, D., Li, G.: Research on economic operation of grid-connected DC microgrid, in Proceedings of International Conference on Renewable Power Generation, Beijing, China, pp. 1-6 (2015)
6. Fan, J.-Y., Zhang, L.: Real-time economic dispatch with line flow and emission constraints using quadratic programming. IEEE Trans. Power Syst. 13(2), 320–325 (1998)
7. Li, Q., Gao, D.W., Zhang, H., Wu, Z., Wang, F.-Y.: Consensus-based distributed economic dispatch control method in power systems. IEEE Trans. Smart Grid. 10(1), 941–954 (2017)
8. Eskandari, M., Li, L., Moradi, M.H.: Improving power sharing in islanded networked microgrids using fuzzy-based consensus control. Sustainable Energy Grids Networks. 16, 259–269 (2018)
9. Meng, L., Dragicevic, T., Roldán-Pérez, J., Vasquez, J.C., Guerrero, J.M.: Modeling and sensitivity study of consensus algorithm-based distributed hierarchical control for DC microgrids. IEEE Trans. Smart Grid. 7(3), 1504–1515 (2015)
10. Yu, M., Song, C., Feng, S., Tan, W.: A consensus approach for the economic dispatch problem in a microgrid with random delay effects. Int. J. Elect. Power Energy Syst. 118, 105794 (2020)
11. Liu, W., Gu, W., Xu, Y., Xue, S., Chen, M., Zhao, B., Fan, M.: Improved average consensus algorithm-based distributed cost optimization for loading shedding of autonomous microgrids. Int. J. Elect. Power Energy Syst. 73, 89–96 (2015)
12. Hu, J., Bhowmick, P.: A consensus-based robust secondary voltage and frequency control scheme for islanded microgrids. Int. J. Elect. Power Energy Syst. 116, 105575 (2020)
13. Zheng, S., Liao, K., Yang, J., He, Z.: Droop-based consensus control scheme for economic dispatch in islanded microgrids. IET Gener., Transm. Distrib. 14(20), 4529–4538 (2020)
14. Zhou, Q., Shahidehpour, M., Alabdulwahab, A., Abusorrah, A.: Privacy-preserving distributed control strategy for optimal economic operation in islanded reconfigurable microgrids. IEEE Trans. Power Syst. 35(5), 3847–3856 (2020)
15. Li, Z., Chen, G.: Distributed fixed-time frequency restoration and economic generation control of droop-controlled microgrids. In 2020 Chinese Automation Congress (CAC), pp. 3175–3180 (2020)
16. Peyghami, S., Davari, P., Mokhtari, H., Blaabjerg, F.: Decentralized droop control in DC microgrids based on a frequency injection approach. IEEE Trans. Smart Grid. 10(6), 6782–6791 (2019)
17. Mortezapour, V., Lesani, H.: Hybrid AC/DC microgrids: A generalized approach for autonomous droop-based primary control in islanded operations. Int. J. Elect. Power Energy Syst. 93, 109–118 (2017)
18. Sabzevari, K., Karimi, S., Khosravi, F., Abdi, H.: Modified droop control for improving adaptive virtual impedance strategy for parallel distributed generation units in islanded microgrids. International Transactions on Electrical Energy Syst. 29(1), e2689 (2019)
19. Siddique, A.B., Munsi, M.S., Sarker, S.K., Das, S.K., Islam, M.R.: Voltage and current control augmentation of islanded microgrid using multifunction model reference modified adaptive PID controller. Int. J. Elect. Power Energy Syst. 113, 492–501 (2019)
20. Azizi, A., Peyghami, S., Mokhtari, H., Blaabjerg, F.: Autonomous and decentralized load sharing and energy management approach for DC microgrids. Electr. Power Syst. Res. 177, 106009 (2019)
21. Tran, Q.T.T., Di Silvestre, M.L., Riva Sanseverino, E., Zizzo, G., Pham, T.N.: Driven primary regulation for minimum power losses operation in islanded microgrids. Energies. 11(11), 2890 (2018)
22. Liu, Y., Deng, W., Yang, P., Teng, Y., Zhang, X., Yang, Y., Pei, W.: Dispatchable droop control strategy for DC microgrid. Energy Rep. 9, 98–102 (2023)
23. Taye, B.A., Choudhury, N.B.D.: A dynamic droop control for a DC microgrid to enhance voltage profile and proportional current sharing. Electr. Power Syst. Res. 221, 109438 (2023)
24. Nutkani, I.U., Loh, P.C., Wang, P., Blaabjerg, F.: Autonomous droop scheme with reduced generation cost. IEEE Trans. Ind. Electron. 61(12), 6803–6811 (2014)
25. Nutkani, I.U., Loh, P.C., Blaabjerg, F.: Cost-based droop scheme with lower generation costs for microgrids. IET Power Electron. 7(5), 1171–1180 (2014)
26. Nutkani, I.U., Loh, P.C., Wang, P., Blaabjerg, F.: Cost-prioritized droop schemes for autonomous AC microgrids. IEEE Trans. Power Electron. 30(2), 1109–1119 (2014)
27. Nutkani, I.U., Loh, P.C., Wang, P., Blaabjerg, F.: Decentralized economic dispatch scheme with online power reserve for microgrids. IEEE Trans. Smart Grid. 8(1), 139–148 (2015)
28. Chen, F., Chen, M., Li, Q., Meng, K., Zheng, Y., Guerrero, J.M., Abbott, D.: Cost-based droop schemes for economic dispatch in islanded microgrids. IEEE Trans. Smart Grid. 8(1), 63–74 (2016)
29. Xin, H., Zhang, L., Wang, Z., Gan, D., Wong, K.P.: Control of island AC microgrids using a fully distributed approach. IEEE Trans. Smart Grid. 6(2), 943–945 (2014)
30. Xu, Q., Xiao, J., Wang, P., Wen, C.: A decentralized control strategy for economic operation of autonomous AC, DC, and hybrid AC/DC microgrids. IEEE Trans. Energy Convers. 32(4), 1345–1355 (2017)
31. Wu, X., Xu, Y., He, J., Wang, X., Vasquez, J.C., Guerrero, J.M.: Pinning-based hierarchical and distributed cooperative control for AC microgrid clusters. IEEE Trans. Power Electron. 35(9), 9865–9885 (2020)
32. Jabr, R.A.: Economic operation of droop-controlled AC microgrids. IEEE Trans. Power Syst. 37(4), 3119–3128 (2021)

33. Nutkani, I.U., Loh, P.C., Blaabjerg, F.: Droop scheme with consideration of operating costs. IEEE Trans. Power Electron. 29(3), 1047–1052 (2013)
34. Dehghani, F., Tourandaz Kenari, M., Shafiyi, M.A.: A novel hybrid droop control strategy for DC microgrid with simultaneous consideration of operating costs and flexibility. International Transactions on Electrical Energy Syst. 31(6), e12896 (2021)
35. Babazadeh-Dizaji, R., Hamzeh, M., Hekmati, A.: A frequency-based economical-sharing strategy for low-voltage DC microgrids. Int. J. Elect. PowerEnergy Syst. 118, 105822 (2020)
36. Hamad, B., Al-Durra, A., EL-Fouly, T.H., Zeineldin, H.H.: Economically optimal and stability preserving hybrid droop control for autonomous microgrids. IEEE Trans. Power Syst. 38(1), 934–947 (2022)
37. Saeidinia, Y., Arabshahi, M., Mousazadeh Mousavi, S.Y., Biglari, M.: Autonomous control of DC microgrid based on a hybrid droop control scheme for total generation cost and transmission power loss reduction. Electrical Engineering. 105(1), 267–283 (2023)
38. Fagundes, T.A., Fuzato, G.H.F., Ferreira, P.G.B., Biczkowski, M., Machado, R.Q.: Fuzzy controller for energy management and SOC equalization in DC microgrids powered by fuel cell and energy storage units. IEEE J. Emerging and Selected Topics in Industrial Electronics. 3(1), 90–100 (2021)
39. Song, S., McCann, R.A., Jang, G.: Cost-based adaptive droop control strategy for VSC-MTDC system. IEEE Trans. Power Syst. 36(1), 659–669 (2020)

How to cite this article: Saeidinia, Y., Arabshahi, M., Aminirad, M., Shafie-khah, M.: Enhancing DC microgrid performance through machine learning-optimized droop control. IET Gener. Transm. Distrib. 1–16 (2024). https://doi.org/10.1049/gtd2.13169

APPENDIX

The parameters of A_{sys}:

$$a_{13} = -k_i H \qquad a_{65} = V_{in_2} / L_2$$

$$a_{14} = -k_i R_{d_1} H \qquad a_{67} = -\left(k_p V_{in_2} H + 1\right) / L_2$$

$$a_{21} = V_{in_1} / L_1 \qquad a_{68} = -\left(k_p V_{in_2} R_{d_2} H\right) / L_2$$

$$a_{23} = -\left(k_p V_{in_1} H + 1\right) / L_1 \qquad a_{76} = 1/C_2$$

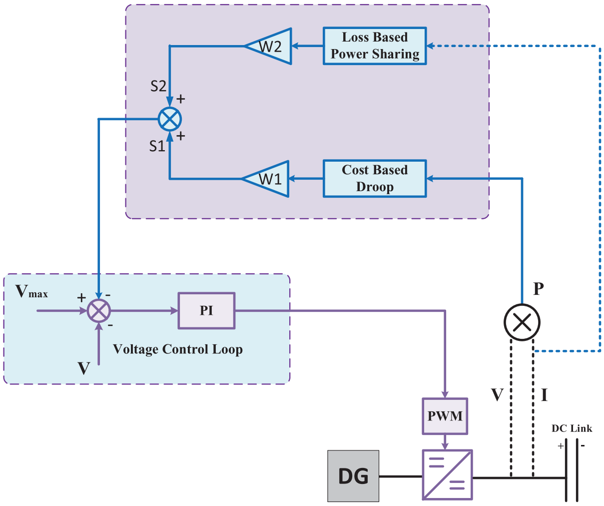

FIGURE A1 The block diagram of the voltage control loop for dispatchable units.

$$a_{24} = -\left(k_p V_{in_1} R_{d_1} H\right) / L_1 \qquad a_{78} = -1/C_2$$

$$a_{32} = 1/C_1 \qquad a_{87} = 1/L_{e_2}$$

$$a_{34} = -1/C_1 \qquad a_{88} = -\left(R_{d_2} + R_{L_2}\right) / L_{e_2}$$

$$a_{43} = 1/L_{e_1} \qquad a_{89} = -1/L_{e_2}$$

$$a_{44} = -\left(R_{d_1} + R_{L_1}\right) / L_{e_1} \qquad a_{94} = 1/C_{dc-bus}$$

$$a_{49} = -1/L_{e_1} \qquad a_{98} = 1/C_{dc-bus}$$

$$a_{57} = -k_i H \qquad a_{99} = -1/RC_{dc-bus}$$

$$a_{58} = -k_i R_{d_2} H$$

Figure A1 outlines the control system employed in our proposed method for DGs. This diagram succinctly illustrates the integration of both IC_D and the loss-based droop methods at the primary control level.

TABLE A1 Simulation parameters of direct current (DC) microgrid (MG).

Part I

Parameters	**Symbolism**	**Value**
Voltages	Voltage reference (V_R)	100 V
	Minimum voltage (V_{Min})	95 V
	Maximum voltage (V_{Max})	105 V
PV	P_{MPPT}	1.6 KW
	C (μF)	330
	L (mH)	0.12
Battery	Nominal battery capacity (C_{bat})	5 Ah
Controllers coefficients	k_{p}	1
	k_{i}	60
Resistive loads	Load#1 (R_1)	1 Ω
	Load#2 (R_2)	0.7 Ω
	Load#3 (R_3)	0.56 Ω
	Load#4 (R_4)	2.05 Ω
	Load#5 (R_5)	2.75 Ω
DC/DC power converters	L (μH)	75
	C (μF)	350
	DC-bus capacitor ($C_{\text{dc-bus}}$)	2000 μF
	Output power	6 KW
	Line inductance (L_{e_j})	100 μH
	Input voltage (V_{in})	48 V
	Switching frequency	50 KHz
	Sensor gain (H)	0.01

Part II

		Coefficients			**Line resistance**
	Unit	$\mathbf{a_{i1}}$	$\mathbf{a_{i2}}$	$\mathbf{a_{i3}}$	R_{Line} **(Ω)**
Cost function and line resistance coefficients	DG1	0.01	0.01	0.004	0.02
	DG2	0.01	0.01	0.004	0.01
	DG3	0.01	0.008	0.002	0.01
	DG4	0.01	0.008	0.005	0.01
	DG5	0.01	0.008	0.002	0.02
	DG6	0.01	0.008	0.005	0.02

Part III

		Scenario 1	**Scenario 2**	**Scenario 3**	**Scenario 4**	**Scenario 5**
Weighting coefficient and loads in different scenarios	W1, W2	0.0, 1	0.02, 0.98	0.01, 0.99	0.13, 0.87	0.25, 0.75
	W3, W4	0.85, 0.15	0.58, 0.42	0.49, 0.51	0.67, 0.33	0.73, 0.27
	W5, W6	0.35, 0.65	0.57, 0.43	0.78, 0.22	0.33, 0.77	0.62, 0.38
	W7, W8	0.88, 0.12	0.91, 0.09	0.81, 0.19	0.8, 0.2	0.98, 0.02
	W9, W10	0.96, 0.04	0.31, 0.69	0.48, 0.52	0.68, 0.32	0.8, 0.2
	W11, W12	0.18, 0.82	0.14, 0.86	0.14, 0.86	0.64, 0.36	0.18, 0.82
	Load	35.5 kW	30 kW	22.5 kW	26 kW	27 kW

Abbreviations: DC, direct current; DG, distributed generation.

TABLE A2 Cost function coefficients and loss resistance for direct current (DC) microgrid (MG) units.

Coefficients				**Line resistance**
Unit	a_{i1}	a_{i2}	a_{i3}	R_{Line} **(Ω)**
DG1	0.01	0.01	0.004	0.02
DG2	0.01	0.01	0.004	0.01
DG3	0.01	0.008	0.002	0.01
DG4	0.01	0.008	0.005	0.01
DG5	0.01	0.008	0.002	0.02
DG6	0.01	0.008	0.005	0.02